Undoped Nanostructures of Zinc Oxide with significant emission properties using Hydrothermal Method

[1]Arunima Bhattacharjee , [2]P. Kamaraj

[1]Department of Chemical Engineering and Materials Science, University of California, Irvine
[2]Department of Chemistry, SRM University,Kattankulathur-603203, Tamil Nadu, India.
Email: : kamaraj97@yahoo.co.in

Abstract- Zinc Oxide Nanoparticles of different size and shapes were prepared using wet-chemical and hydrothermal method. Novel nanostructures with better emission properties compared to the wet-chemical synthesis have been successfully produced by hydrothermal route. However the size of the structures was more confined in the wet-chemical synthesis. In the nanorods synthesized via hydrothermal route, visible light emission of very high intensity has been observed in the red emitting region around 650nm. None of the structures have been doped and hence the emission can be attributed to the various substructure attachments to the rods. Chemical synthesis methods yield rods with unfinished ends. The growth direction is found to be (0001) in the hexagonal rods with hexagon like sub-structures attached to them. The structural, chemical and optical properties of the samples have been studied using X-ray diffraction (XRD), scanning electron microscopy (SEM), energy dispersive X-ray (EDX) analysis; Fourier transformed infrared (FTIR) spectroscopy and UV–VIS spectroscopy.

Key Words: wet- chemical method, hydrothermal, nanorods, hexagonal, sub-structures.

I. INTRODUCTION

Zinc Oxide is a versatile material that possesses many unique characteristics like high-specific surface area, non-toxicity, chemical stability, electrochemical activity, and high electron communication features[1-5]. Among these oxides, ZnO exhibits the most diverse and abundant configurations of nanostructures known to date, such as nanocombs, seamless nanorings, aligned nanopropellers, nanohelixes/nanosprings, nanobows, nanobelts (NB), nanowires (NW), and nanocages [6]. Fundamental research into functional oxide-based one-dimensional nanostructures is in rapid progress due to their unique and novel applications in optics, optoelectronics, catalysis, and piezoelectricity [6,7,8]. Wide band gap semiconducting oxides with nanostructures such as nanospheres, nanorods, nanowires are of particular interest [9]. Out of many semiconducting oxides, the wurtzite family of structures has few important members, such as ZnO, GaN, AlN, ZnS, CdSe, which are important materials for the above mentioned applications [6]. ZnO is a typical member of the wurtzite family of structures [6]. It has a wide band gap (*Eg*=3.37 eV) [10, 11] and a large exciton binding energy of 60 MeV [12,13], significantly higher in comparison to materials of the same family as GaN, ZnSe etc. [10] and is a photochemical semiconductor [14-17]. ZnO nanostructures exhibit high catalytic efficiency and strong adsorption ability apart from the other advantages of the wurtzite family of nanostructures. Research on ZnO nanoparticles doped with different metal atoms is of great significance [11]. It is usually reported that the UV emission properties in undoped Zinc Oxide nanoparticles are weaker than doped ones [11] and hence doping of the nanoparticles is preferred to obtain novel properties.

In the present work, high quality undoped nanorods of zinc oxide with attached hexagonal substructures to the body of the rods has been synthesized. The structures are novel and have not been reported elsewhere. The hydrothermal method of synthesis route was followed and a comparison has been made with the wet-chemical synthesis route. These structures have been characterised by powder XRD, HRSEM, and UV-Vis spectrophotometer.

II. EXPERIMENTAL MATERIALS AND METHODS

All the chemicals (analytical grade reagents) were used without further purification. In a typical experiment, 8.9g(0.03 mols) of Zinc nitrate was thoroughly dissolved in 30ml Millipore water and 1.6g(0.04 mols) of sodium hydroxide was dissolved in 20ml Millipore water. The pH of the second solution was measured to be 13.5. This solution was allowed to add drop wise to the Zinc Nitrate solution until the pH was adjusted to 10. This was done under constant stirring in a magnetic stirrer and the solution was left under vigorous stirring for three hours after which it was centrifuged and washed with DI water. The powder was dried at 60 degrees for several hrs. This is denoted as sample 1. A similar

experiment was done under the same pH conditions as the one described above. The reagent quantities were same. The solution mixture was allowed to stir for 2 hrs and then was put in a 50ml teflon lined autoclave and heated at 150 degrees for 3 hrs. The powder was dried at 60 degrees for several hrs. This is denoted as sample 2. To see the effect of change in precursor and solvent on morphology another experiment was performed. 6.8g (0.03 M) of Zinc Acetate was dissolved in 30ml Ethanol. To this was added 20ml of a 2M solution of sodium hydroxide in Ethanol. The solution was left under vigorous stirring for 3 days after which it was washed with ethanol and dried at room temperature. This is denoted as sample 3. In all the experiments PVP was used as a surfactant to reduce the grain size and provide stability.

Characterizations

The crystalline structure of the dried powders were analysed by powder X-ray diffraction. The powder X-ray diffraction (PXRD) was carried out on a Xpert Pro X-ray diffractometer using Cu K_α -1 radiation (λ = 0.1406 nm) in Bragg–Brentano geometry. The specimen for PXRD was prepared by pressing the dry powder in a groove scooped onto a quartz plate. Diffraction data were collected at a scan rate of 1.2°, 2θ per minute. Prior to measurements, the PXRD machine was calibrated using a certified α – quartz specimen.

The chemical composition and stoichiometry of ZnO deposits were analyzed by energy dispersive X-ray analysis as well. The as-synthesized nanocrystalline ZnO powder samples were used as samples for EDAX analysis. The EDAX analysis was done using the set-up integrated with a scanning electron microscope (SEM) (Jeol Japan Inc., Model: JSM 6060) and high resolution scanning electron microscope (HRSEM) (ZEISS, Japan). The EDAX analysis was carried out at several locations on the powder sample and deposits in order to check the exact composition and stoichiometry. Compositions indicated retention of particle stoichiometry in powder sample as well as deposits.

UV-Vis absorption spectroscopic analysis of ZnO was carried out using a double Beam spectrophotometer. Optical absorption spectrum of the Zinc Oxide powder in the UV-Visible range was obtained by running a colloidal suspension in analytical grade ethanol as the sample and pure ethanol as reference.

III. RESULTS AND DISCUSSIONS

The phase and purity of all the prepared ZnO samples were determined by X-Ray Powder Diffraction. A typical X-Ray powder diffractogram(XRD) of the three ZnO samples are shown in the figure 1(a) and 1(b). The XRD measurement reveals that the nanoparticles have hexagonal wurtzite sturcture. The latice constants obtained by calculation from the data matches with the JCPDS card no. of bulk ZnO. For all the samples no extra peaks from other impurities were found. In both the wet- chemically prepared samples as can be seen in fig 1(a) a slight broadening of the peaks were seen. Further it can be noticed that the (200), (112) and (201) peaks are not completely separated in these two samples and also the peaks are broad which indicates the nanocrystalline nature of the samples [18]. In the third sample (fig 1(b)) that had been prepared via hydrothermal method however the peaks have greater intensity and all peaks are well separated. Figure 1(c) shows the EDX pattern of this third sample which shows 100% purity.

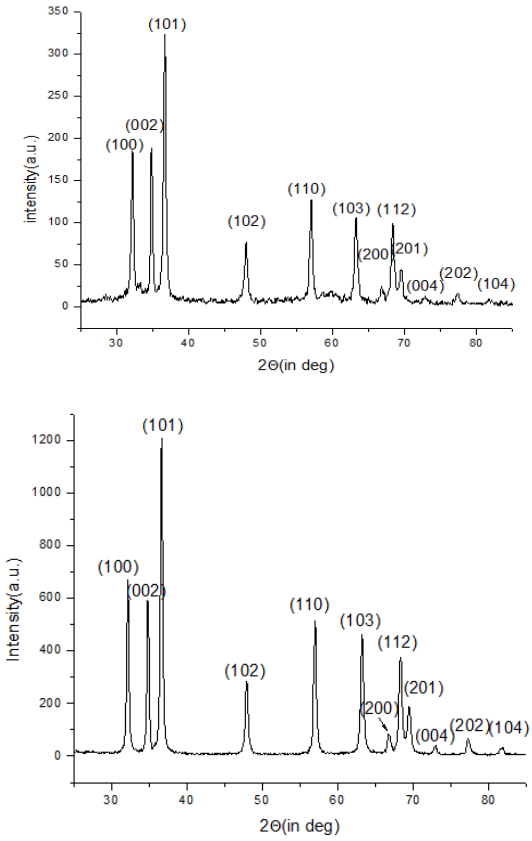

Figure 1(a): X-Ray Diffraction pattern of wet-chemically prepared sample 1 and 3 in order.

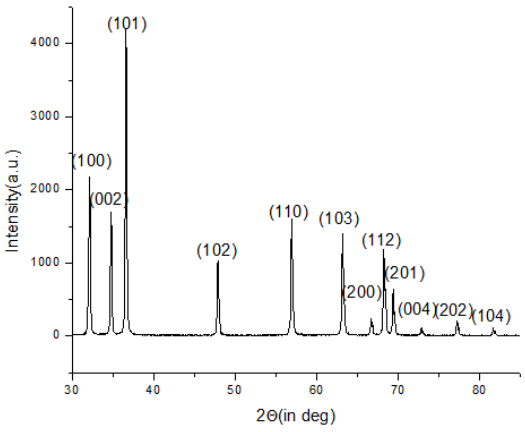

Figure 1(b): X-Ray Diffraction pattern of hydrothermally prepared sample 2

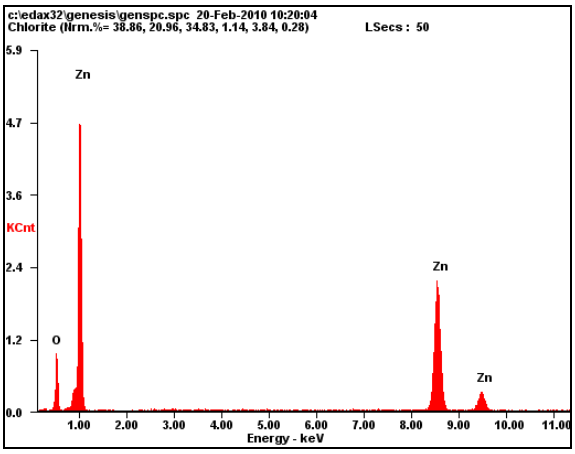

Elements	Atomic Composition
Zn	43.25%
O	56.75%

Figure 1(c): EDX of sample 3

Scanning Electron Micrograph of sample 1 and sample 2 reveals nanorods even though in both the cases the morphologies of the rods are different. As shown in the figure 2 the nanorods in sample 1 are with broken and unfinished ends. The diameter of these rods is around 20 nm. This varies widely with sample 2 as is shown in figure 3. The nanorods here are perfected hexagonal structures with a length of more than 2 □m and a diameter of 500nm. These structures further have hexagon sub-structures attached along the body of the rod as is seen in the fig 3. The growth direction can be attributed to the pH conditions. The attachment of the sub-structures must be externally at a later time after the growth of the rod was completed.

In the case of sample 3 the Scanning Electron Micrograph (fig 4) shows nanorods of much smaller dimensions and a few spherical particles also. The smaller dimensions and morphology can be attributed to longer mechanical stirring time and surfactant effect as has been suggested [19]. However with the change of precursor a distinct change is seen in the morphology of the samples.

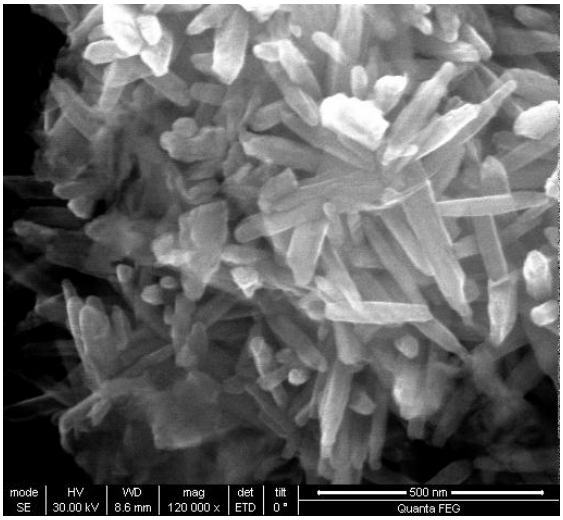

Figure 2: SEM images of sample 1

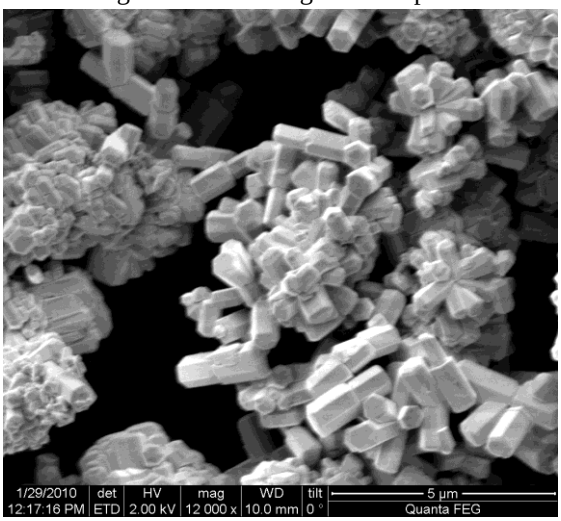

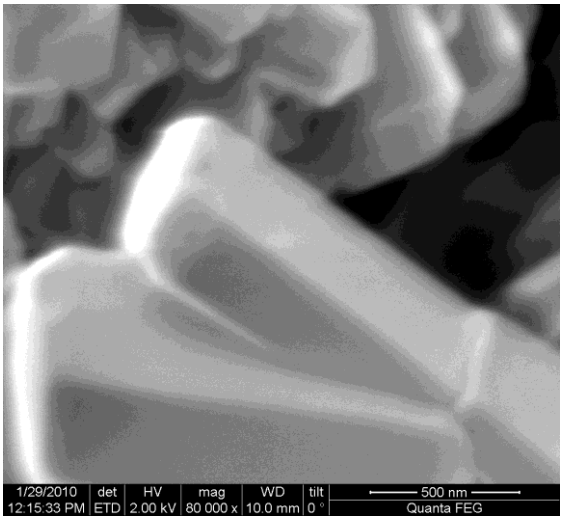

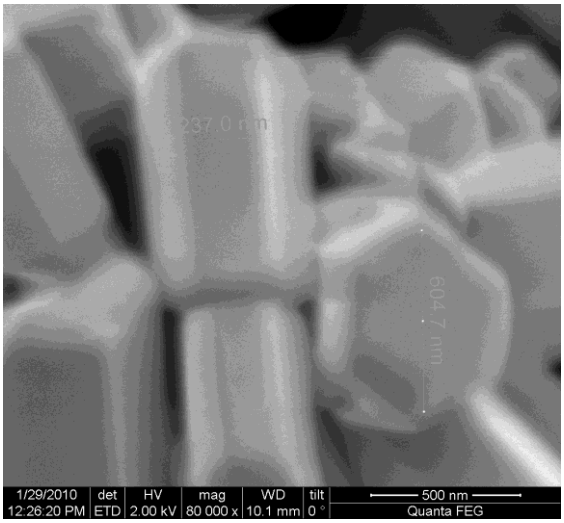

Figure 3: SEM images of sample 2

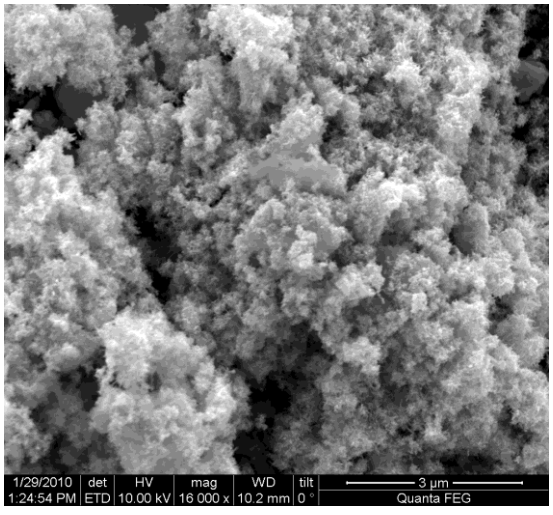

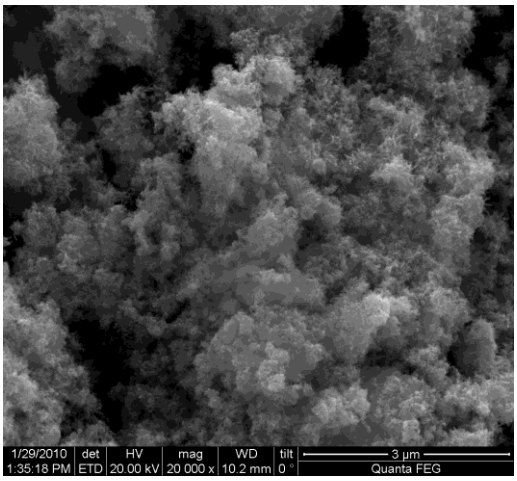

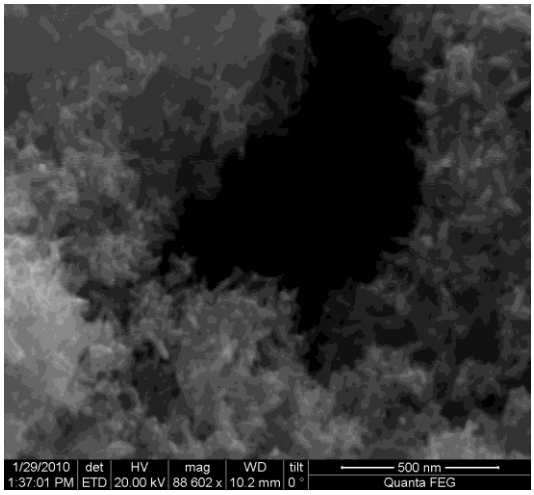

Figure 4: SEM images of sample 3

The optical absorption of the ZnO samples is shown in the figure 5. The optical absorbance was recorded at room temperature by a double beam spectrophotometer. It is evident from the figure 5(a) that sample 1 exhibits strong absorption at 364 nm as is indicated.

In the case of sample 3(fig 5(b)) a strong absorption peak is observed at 367 nm and a hump at 259nm. The appearance of two peaks can be attributed to the presence of rods and spherical particles in the sample as has been confimed in the SEM data. The peak at 367nm is caused due to the longitudinal vibration of the surface plasmons along the length of the rods while the peak at 259nm is due to the transverse vibration in the spherical nanoparticles. There is also appearance of a small edge after the 259nm peak. This can be attributed to the vibration of the surface plasmons along the diameter of the rods. The blue shifting of the edge shows confinment along the diameter [20].

The absorbance recorded for sample 2(fig 5(c)) shows a sharp peak at 382nm and an edge at after 250nm. Further this sample shows a high intensity broad peak at 647nm which is in the red emitting region usually obtained by doping of ZnO with other impurity atoms. However sample 2 is pure Zinc Oxide as can be seen from the EDX analysis. This emission can hence be attributed to the sub-structure attachments along the

body of the rods as can be seen in the SEM image in figure 2. The peak at 382nm can be attributed due to vibration of the surface plasmons along the length and the edge is due to the vibrations along the diameter of the rods. The edge is blue-shifted due to confinement along the diameter [20].Another reason that can be attributed to the broad peak is the presence of hydrogen atoms in the lattice of ZnO in the sample.The presence of oxygen vacancies can be ruled out in this case as we can deduce from the EDX result that there is a presence of excess oxygen due to the synthesis being carried out in an oxygen reach atmosphere. The presence of PVP surfactant was detected by FT-IR spectra [21] which gave a peak at 1658 cm^{-1}.

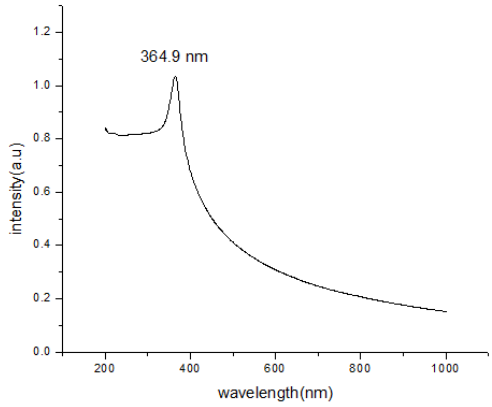

Figure 5(a): UV-Vis absorption of sample 1

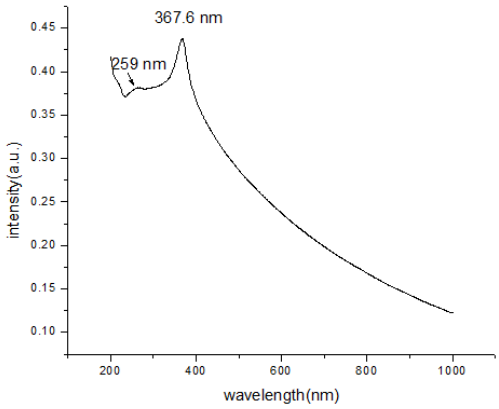

Figure 5(b): UV-Vis absorption of sample 3

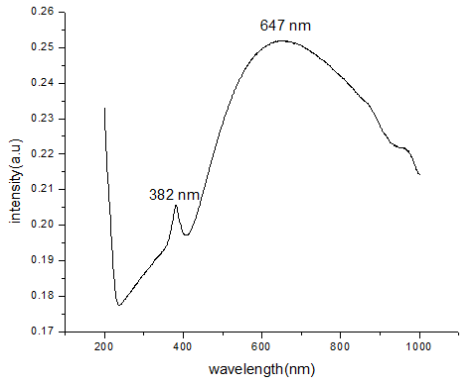

Figure 5(c): UV-Vis absorption of sample 2

IV. CONCLUSION

Wurtzite ZnO nanoparticles were prepared both in alcohol and aqueous media. PVP was used as a surfactant to control the size and shape of the nanoparticles. This study describes a novel methodology to synthesize undoped nanorods with better emission properties which can usually be achieved only by doping. The structures also are newly reported as can be seen from the HRSEM images. Quantum size effects are seen in the nanorods as is evident from the optical properties.

V. ACKNOWLEDGEMENTS

The authors would like to acknowledge SRM University for various characterisation facilities including XRD, SEM, UV-Vis Spectrophotometer and FT-IR. The authors also like to thank IIT Madras, SAIF for providing EDX facility.

VI. REFERENCES

[1] Kodihalli G. Chandrappa et al, (2009), A Hybrid Electrochemical-Thermal Method for Preparation of Large ZnO Nanoparticles, J Nanopart Res , DOI 10.1007/s11051-009-9846-0.

[2] Femg YJ, Ming LY, Wei LH, Chun LY, Hui LB, Wu FX et al (2005) Growth and properties of ZnO nanotubes grown on Si(1 1 1) substrate by plasma-assisted molecular beam epitaxy. J Cryst Growth 280:206–211.

[3] Zhao QX, Willander M, Morjan RE, Hu QH, Campbell EEB (2003) Optical recombination of ZnO nanowires grown on sapphire and Si substrates. Appl Phys Lett 83:165–167.

[4] Meulenkamp EA (1998) Synthesis and growth of ZnO nanoparticles. J Phys Chem B 102:5566–5572.

[5] Roy VAL,Djuris˘ic AB, ChanWK, Gao J, LuiHF, Surya C (2003) Luminescent and structural properties of ZnO nanorods prepared under different conditions. Appl Phys Lett 83:141–143.

[6] Zhong Lin Wang(2004), Zinc Oxide Nanostructures: growth properties and applications, J. Phys.: Condens. Matter **16** : R829–R85.

[7] V. A. Coleman and C. Jagadish(2006), Basic properties and applications of ZnO,

[8] Vayssieres L (2003), Growth of arrayed nanorods and nanowires of ZnO from aqueous solutions, Adv Mater 15: 464–466.

[9] Jong PiL KIM et al,(2010), Characteristics of ZnO Nano-Crystals Grown on Al-doped ZnO Thin Films Deposited by using the PLD

Method, Journal of the Korean Physical Society, Vol. 56, No. 1, 378-382.

[10] Xiang Liu et al(2004), Growth mechanism and properties of ZnO nanorods synthesized by plasma-enhanced chemical vapor deposition, Journal of Applied Physics, Vol. 95, No. 6, DOI: 10.1063/1.1646440.

[11] Hui Li et al, (2009), Effects of In and Mg doping on properties of ZnO nanoparticles by flame spray synthesis, J Nanopart Res , Vol No. 11,917–92.

[12] J. H. Yang, J. H. Zheng, H. J. Zhai, L. L. Yang, L. Liu, M. Gao(2009), Solvothermal growth of highly oriented Wurtzite- structured ZnO nanotube arrays on Zinc foil., Cryst. Res. Technol. 44, No. 6, 619 – 623,DOI 10.1002/crat.200800633

[13] Chia Ying Lee, Tseung Yuen Tseng, Seu Yi Li, Pang Lin (2003), Growth of Zinc Oxide Nanowires on Silicon (100)., Tamkang Journal of Science and Engineering, Vol. 6, No. 2, 127-132.

[14] Yan Z (2003) Nanocrystalline catalytic technology. Chemical Industrial Press, Beijing, p 68

[15] Hengxiang G, Yunyao H, Qifeng W, Guojuan J, Zebo F, Yinyue W (2004) Polycrystalline ZnO films deposited on glass by RF reactive sputtering. Semicond Photonics Technol 10(2):97–100

[16] Xitang Z, Jiaqi Z, Jinjie X, Tengfeng X, Dejun W, Yubai B, Tiejin L, Jiannian Y (1999) Studies of surface photovoltage spectroscopy on quantum-sized ZnO nanoparticles. Chem J Chin Univ 20(12):1945–1947

[17] Caijun X (2003) Nanocrystalline build material. Chemical Industrial Press, Beijing, pp 51–51

[18] P. Kumbhakar, D. Singh, C.S. Tiwary, A. K. Mitra (2008), Chemical Synthesis and Visible Photoluminesence emission from Monodispersed ZnO Nanoparticles., Chalcogenide letters, Vol 5, No. 12, 387-384.

[19] Ali Elkhidir Suliman, Yiwen Tang, Zhan Xing, Zhijie Jia, (2006), The effect of PVP addition and Heat Treatment On Zinc oxide nanoparticles., Journal of Applied Sciences 6 (6), 1298-1301.

[20] Doungporn Yiamsawas, Kanittha Boonpavanitchakul, Wiyong Kangwansupamonkon(2009), Preparation of ZnO Nanostructures by Solvothermal Method, Journal of Microscopy Society of Thailand 2009, 23(1), 75-78.

[21] Shriwas S Ashtaputre et al, (2005), Synthesis and analysis of ZnO and CdSe nanoparticles, Journal of Physics, Vol. 65, No. 4, 615-620.

◈◈◈